Molecular Crystals and Liquid Crystals

Publication details, including instructions for authors and subscription information:
http://www.tandfonline.com/loi/gmcl20

Optical Angular Momentum Flux in Liquid Crystals

Bruno Piccirillo [a]

[a] Dipartimento di Scienze Fisiche and INFM, Sezione di Napoli, Università di Napoli "Federico II", Monte S. Angelo, via Cintia, Napoli, Italy

Version of record first published: 31 Aug 2006

To cite this article: Bruno Piccirillo (2005): Optical Angular Momentum Flux in Liquid Crystals, Molecular Crystals and Liquid Crystals, 429:1, 133-147

To link to this article: http://dx.doi.org/10.1080/15421400590930863

Mol. Cryst. Liq. Cryst., Vol. 429, pp. 133–147, 2005

ISSN: 1542-1406 print/1563-5287 online
DOI: 10.1080/15421400590930863

Taylor & Francis
Taylor & Francis Group

Optical Angular Momentum Flux in Liquid Crystals

Bruno Piccirillo
Dipartimento di Scienze Fisiche and INFM, Sezione di Napoli, Università di Napoli "Federico II", Monte S. Angelo, via Cintia, Napoli, Italy

In this paper the role played by the angular momentum of light in the optical reorientation of a nematic liquid crystal was studied in the case of a normal incident elliptically shaped laser beam with circular polarization. Above the threshold power for the OFT, the molecular director suffered a stationary reorientation due to the balance between the orbital and spin angular momentum of light transferred to the sample. The director started to rotate only above a second threshold power. The experimental results qualitatively matched theoretical predictions.

Keywords: angular momentum; liquid crystals; nonlinear optics

INTRODUCTION

In the last two decades liquid crystals, in the framework of nonlinear optics research, have been proved to be able to exchange with photons both intrinsic (or spin) and orbital angular momentum. This way started in 1986 along the lines of a celebrated experiment by Beth [1], when the collective rotation of liquid crystal molecules in the field of a normally incident circularly polarized laser beam was observed [2]. This phenomenon was explained in terms of a Self-Induced Stimulated Light Scattering (SISLS) process where a transfer of spin angular momentum from the beam to the sample was involved [3]. In the SISLS process it is the *change* in the photon angular momentum that is transferred to matter. This is a distinctive difference between the

I thank MIUR (Ministero dell'Istruzione, Università e Ricerca) and INFM (Istituto Nazionale per la Fisica della Materia). Special thanks are to Prof. Enrico Santamato for enlightening discussions and valuable advices.

Address correspondence to Bruno Piccirillo, Dipartimento di Scienze Fisiche and INFM, Sezione di Napoli, Universita di Napoli "Federico II", Monte S. Angelo via Cintia, 80126, Napoli, Italy. E-mail: piccirillo@na.infn.it

SISLS and the transfer of angular momentum by photon absorption. When the photon angular momentum is to be transferred to matter in an absorption process, the incident photons must be already prepared in a state with non-zero angular momentum. On the contrary, in the SISLS process the angular momentum transfer can take place even when the incident light carries no angular momentum at all. The SISLS process was recognized to be the physical grounds for complex dynamical regimes [4,5] and for operating light-driven molecular motors [6]. Exploiting the same principle, manipulation of small transparent and birefringent particles trapped by optical tweezers was also achieved [7].

The photon orbital angular momentum transfer to matter is a more recent issue. The first direct observation of orbital momentum transfer was performed on absorptive particles trapped in the dark central minimum of a doughnut laser beam [8]. The extension to transparent bodies was first made in liquid crystals, using a normally incident unpolarized or linearly polarized laser beam with elliptical cross-section at the sample position [9]. A homeotropically aligned nematic film, irradiated by an astigmatic laser beam, carrying zero-average orbital angular momentum, behaves as an astigmatic lens mode converter, which realizes the orbital angular momentum transfer. This experiment realized the orbital counterpart of SISLS and put into practice an idea coming from a theoretical work by Allen *et al.* [10] according to which the measurement of the mechanical torque arising from the orbital angular momentum was to be performed from Beth's experiment mould. In such an experiment, the astigmatism of the optical system stands for the birefringence of the retardation plate in Beth's experiment. This picture was supported by approximate calculations made either assimilating the liquid crystal sample to a birefringent plate with a Gaussian shaped retardation profile in the transverse plane [9] or exploiting Ritz's variational method to the liquid crystal free energy functional [11]. Although very approximate, both approaches lead to the idea that the spin part of the light angular momentum directly couples with the molecular director $\boldsymbol{n}(\boldsymbol{r}, t)$ and the orbital part with the gradients of $\boldsymbol{n}(\boldsymbol{r}, t)$. The simultaneous transfer of both the orbital and the spin angular momentum leads, among other things, to complex dynamics of $\boldsymbol{n}(\boldsymbol{r}, t)$ [9,12,11], to deterministic chaos and on-off intermittency [13] and to all optical multistability [11].

In the present paper the simultaneous transfer of spin and orbital angular momentum is faced in the special case of a circularly polarized laser beam with elliptical cross-section at the sample position. For a circularly shaped laser beam, experimental conditions reproduce

those for the well-known SISLS [3,15] due to the photon spin angular momentum. Using an astigmatic laser beam, SISLS process takes very peculiar features unambiguously explainable in terms of the simultaneous and competitive transfer of spin and orbital angular momentum. The optical inhomogeneity of the molecular collective allows for an additional torque superimposing to the volume optical torque

$$\boldsymbol{\tau}_o = (1/8\pi)\mathrm{Re}[\boldsymbol{D} \times \boldsymbol{E}^*] = (\epsilon_a/4\pi)\langle \boldsymbol{D} \times \boldsymbol{E} \rangle. \tag{1}$$

In the following sections, deviations from the cylindrically symmetric ordinary geometry are emphasized and a simple model for data analysis is also presented.

TRANSFER OF PHOTON ANGULAR MOMENTUM TO LIQUID CRYSTALS

Starting from the general equations for the motion of the liquid crystalline fluid, general angular momentum conservation theorems have been recently deduced, allowing for a deeper insight into the mechanism of the light angular momentum transfer to liquid crystals [14]. The explicit expressions of conservation theorems, upon integration over a slab V perpendicular to the propagation direction $\boldsymbol{z}$ of the light beam, in the paraxial approximation, are

$$\int_V \rho(\boldsymbol{r} \times \dot{\boldsymbol{v}}) \cdot \boldsymbol{z}\, d\boldsymbol{r} = \oint_{\partial V} \boldsymbol{z} \cdot \hat{\boldsymbol{L}} \cdot \boldsymbol{z}\, ds - \int_V \boldsymbol{w}^e \cdot \boldsymbol{z}\, d\boldsymbol{r} + \int_V (\boldsymbol{r} \times \boldsymbol{f}^v) \cdot \boldsymbol{z}\, d\boldsymbol{r} \tag{2}$$

$$\int_V I(\boldsymbol{n} \times \ddot{\boldsymbol{n}}) \cdot \boldsymbol{z}\, d\boldsymbol{r} = \oint_{\partial V} \boldsymbol{z} \cdot \hat{\boldsymbol{S}} \cdot \boldsymbol{z}\, ds + \int_V \boldsymbol{w}^e \cdot \boldsymbol{z}\, d\boldsymbol{r} + \int_V \boldsymbol{\tau}^v \cdot \boldsymbol{z}\, d\boldsymbol{r}, \tag{3}$$

where ρ is the liquid crystal density, I is the momentum of inertia per unit volume associated to the rotation of $\boldsymbol{n}(\boldsymbol{r}, t)$, $\boldsymbol{v}$ is the liquid crystalline fluid velocity, $\boldsymbol{w}^e$ is the antisymmetric part of the elastic stress tensor, $\boldsymbol{f}^v$ is the viscous force per unit volume acting on the fluid, $\boldsymbol{\tau}^v$ is the viscous torque per unit volume acting on the fluid, $\hat{\boldsymbol{L}}$ and $\hat{\boldsymbol{S}}$ respectively are the electromagnetic orbital and spin angular momentum flux densities inside the liquid crystalline material. In such a general framework, the coupling between the orbital angular momentum and the gradient of $\boldsymbol{n}(\boldsymbol{r}, t)$ came out when inertial terms are neglected and the fluid velocity $\boldsymbol{v}$ set approximately to 0.

Regarding the nematic sample as a thin birefringent plate with an astigmatic gaussian-shaped phase profile, the paraxial expression for

the spin angular momentum transferred per second turns out to be [12]

$$\Delta S_z = -\frac{1}{\omega}\int dx\, dy\, I(x,y)\Delta s_3(x,y) \tag{4}$$

where $I(x,y)$ is the intensity profile of the beam, ω is the optical frequency, and Δs_3 is the change suffered by the reduced Stokes' parameter $s_3 = 2\mathrm{Im}(E_x E_y^*)/(|E_x|^2 + |E_y|^2)$ in traversing the medium ($s_3 = \mp 1$ for left/right handed polarization, respectively, and $s_3 = 0$ for linear polarization). Integration is carried out across the transverse plane. Let us notice that Eq. (4) is consistent with the optical torque (1).

Analogously, the orbital angular momentum transferred to NLC film per second is [12]

$$\Delta L_z = \frac{1}{\omega}\int dx\, dy\, I_e(x,y)(\boldsymbol{r}\times\nabla)_z \Delta\Psi_e(x,y). \tag{5}$$

where, in the case of NLCs, $I_e(x,y)$ and $\Delta\Psi_e(x,y) = \Psi_e(x,y,L) - \Psi_e(x,y,0)$ are the intensity profile and the phase change of the extraordinary wave, respectively. ΔL_z depends on the gradients of the phase change $\Delta\Psi_e(x,y)$ and, hence, on the gradients of $\boldsymbol{n}(\boldsymbol{r},t)$. Equation (5) provides a new source of optical torque. The expression (5) for ΔL_z may be obtained using the prescriptions of Quantum Optics: each photon in the incident beam has orbital angular momentum $l_z = \hbar(\boldsymbol{r}\times\boldsymbol{k})_z$, where $\boldsymbol{k}$ is the wavevector. In the paraxial approximation, $\boldsymbol{k} = \nabla\Psi$, where Ψ is the optical phase.

The conservation theorems expressed by Eqs. (2) have already been obtained in a simple case in Ref. [12], starting from a free energy functional shaped on the grounds of the following experimental situation. A laser beam is focused at normal incidence onto an NLC film of thickness L and produces at the sample position a Gaussian intensity profile with different waists w_x and w_y (without loss of generality we may take $w_x > w_y$):

$$I(x,y) = I_0\ \mathrm{e}^{-\left(\frac{x^2}{w_x^2}+\frac{y^2}{w_y^2}\right)}. \tag{6}$$

The beam phase profile is assumed to be uniform over the beam cross section. The beam is circularly polarized. The molecular alignment at the sample walls is assumed homeotropic. For a beam with circular cross-section, $w_x = w_y$, the experimental geometry reduces to the well-known case where collective precession of the molecules in the

film has been observed above the threshold for the Optical Fréedericksz Transition (OFT) [2]. We expect, therefore, that also in the present case no reorientation takes place in the sample until the intensity I_0 at the center of the beam reaches a threshold value. Very close to the threshold, the laser-induced reorientation is very small, so that we may assume $n_z \simeq 1$ and consider n_x and n_y small quantities. In view of the homeotropic boundary conditions at $z = 0$ and $z = L$, we may take

$$\begin{aligned} n_x &= n_x(x,y,t)\sin\left(\frac{\pi z}{L}\right) = \theta(x,y,t)\cos\phi(t)\sin\left(\frac{\pi z}{L}\right) \\ n_y &= n_y(x,y,t)\sin\left(\frac{\pi z}{L}\right) = \theta(x,y,t)\sin\phi(t)\sin\left(\frac{\pi z}{L}\right) \\ n_z &\simeq 1, \end{aligned} \tag{7}$$

where $\theta(x,y,t)$ is the small angle between $\boldsymbol{n}(\boldsymbol{r},t)$ and the z-axis. As no boundary conditions are imposed on the azimuthal angle ϕ, Eqs. (7) assume that $\phi(t)$ is uniform in the transverse plane. Because of the homeotropic alignment imposed by the walls, n_x and n_y vanish outside the elliptically illuminated region, so that $\theta(x,y,t)$ may be assumed to have a Gaussian elliptical profile too:

$$\theta(x,y,t) = \theta_m(t)\mathrm{e}^{-\frac{1}{2}G_{ij}(t)x_i x_j}, \tag{8}$$

where $G_{ij}(t)$ is a 2×2 time-dependent positive definite symmetric matrix. The matrix $G_{ij}(t)$ has three independent components uniquely related to the major axis length $\theta_1(t)$, the minor axis length $\theta_2(t)$, and the angle $\gamma(t)$ between the reference x-axis and the major axis of the θ-profile. In this way, the whole reorientation in the sample is parametrized by five time-dependent quantities, each having a simple physical meaning: $\theta_m(t), \phi(t), \gamma(t), \theta_1(t), \theta_2(t)$. A closed set of first order Ordinary Differential Equations (ODEs) for these parameters adding to the Euler-Lagrange equations derived from the free energy $\mathcal{F} = \int F\, dx\, dy$ a viscous term, such as $(-\dot{n}_x, -\dot{n}_y)$, where the dot means derivative with respect to the reduced time $\tau = (k_{33}/\gamma_1 L^2)t$, k_{33} being the bend elastic constant and γ_1 the effective viscosity coefficient [11,12]. A relevant outcome of such a picture is that the photon spin and orbital angular momenta act on different degrees of freedom of the NLC. The spin, in fact, is seen to be coupled with the time derivative $\dot{\phi}(t)$ of the azimuthal angle $\phi(t)$ of $\boldsymbol{n}(\boldsymbol{r},t)$, while the orbital angular momentum with the time derivative $\dot{\gamma}(t)$ of the angle $\gamma(t)$ defining the orientation of θ-distribution. The angles $\phi(t)$ and $\gamma(t)$, however, turn out to be coupled to each other by an elastic term proportional to $(k_{11} - k_{22})$, where k_{11} and k_{22} are the splay and twist elastic constants

respectively. This elastic coupling tends to align the $\phi(t)$ angle with the major axis of θ-distribution and it is internal to the NLC. Such an elastic coupling tends to disappear as $\theta_1(t) - \theta_2(t)$ tends to zero, i.e. when the liquid-crystalline equivalent lens becomes spherical. Besides, the internal elastic coupling vanishes also in the one-elastic-constant approximation. This approximation, although widespread in literature, is inadequate in the present case [16,17].

The counterparts of Eqs. (2) finally are

$$\Delta L_z = \gamma_1 \int_0^L dz \int dx\, dy \sum_{i=1}^{2} \dot{n}_i (x\partial_y - y\partial_x) n_i - (k_{11} - k_{22}) \int_0^L dz \int dx\, dy\, (\partial_x n_x + \partial_y n_y)(\partial_x n_y - \partial_y n_x), \quad (9)$$

where ΔL_z is given by Eq. (5), and

$$\Delta S_z = -\gamma_1 \int dx\, dy\, (n_x \dot{n}_y - n_y \dot{n}_x) + (k_{11} - k_{22}) \int_0^L dz \int dx\, dy\, (\partial_x n_x + \partial_y n_y)(\partial_x n_y - \partial_y n_x), \quad (10)$$

where ΔS_z is given by (4).

THE EXPERIMENT

In the experiment the sample was a 50 μm thick E7 nematic film sandwiched between glass covers coated with DMOAP for homeotropic alignment. The sample was pumped by a frequency-doubled c.w. Nd:YAG laser source, working at $\lambda = 532$ nm. Two cylindrical lenses, assembled in the inner confocal configuration with their axes orthogonal to each other, were used to obtain an elliptical beam waist at the sample position. The focal lengths of the lenses were $f_x = 500$ mm and $f_y = 30$ mm in the x and y directions respectively. The beam radii in the common focal plane were found to be $w_x = 130\,\mu$m and $w_y = 10\,\mu$m, corresponding to a profile ellipticity $e \equiv w_x/w_y = 10$. Circular polarization was obtained previous a birefringent quarter waveplate.

The detection apparatus provides simultaneous and real time measurements of the angular aperture Θ and of the average polarization direction angle Φ of the far-field self-diffraction pattern, which are formed beyond the LC sample when reorientation takes place [5]. For small LC distortion one approximately has $\Theta(t) \propto \theta^2(t)$ and $\Phi \simeq \phi(t)$, where $\theta(t)$ and $\phi(t)$ are the polar coordinates of the molecular director

$\boldsymbol{n}(\boldsymbol{r},t)$, averaged over the sample [5]. The angles $\Theta(t)$ and $\Phi(t)$ provide roughly independent degrees of freedom for $\boldsymbol{n}(\boldsymbol{r},t)$.

The present work is basically aimed at investigating the deviations induced by the photon orbital angular momentum transfer to the rotation of the molecular director driven by the photon spin. The geometry of the experiment with circularly polarized light resembles in some ways the one faced with unpolarized light [9,18]: no favourite direction exists with the exception of the major axis of the laser beam transverse profile at the sample position. However, differently from the case of unpolarized light and from the case of linearly polarized light [9,11,12], now the pumping laser beam does carry a spin angular momentum of its own ($\pm\hbar$ per photon wether left- or right-circularly polarized), though it continues carrying zero average orbital momentum.

In Figure 1 the time averaged value of θ_m^2 is reported as a function of the incident power P. Below the pump critical power $P_{th}^c = (314 \pm 4)$ mW, no effect was observed and the light transmitted beyond the

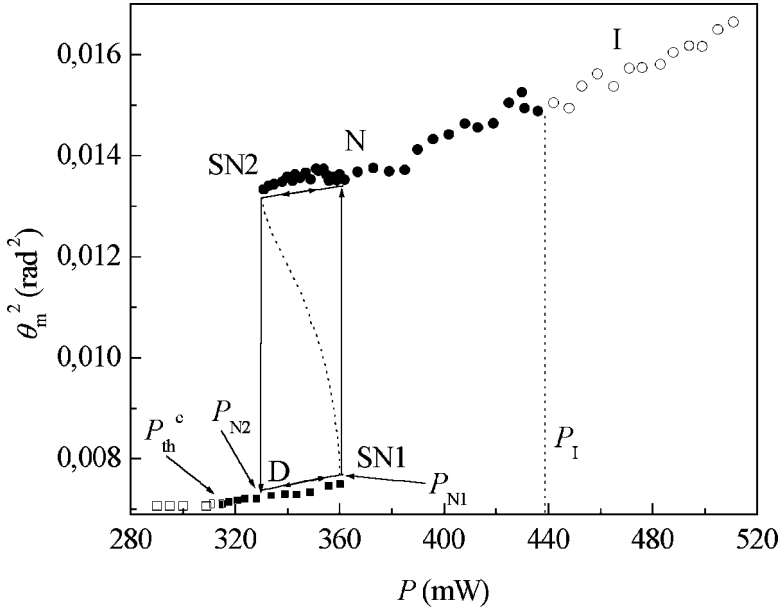

FIGURE 1 Time averaged θ_m^2 as a function of the incident power for circularly polarized light. The experimental points are distinguished as follows: □ undistorted states; ■ distorted steady states; ● nutating states; ○ intermittent oscillations. The critical values $P_{th}^c, P_{N1}, P_{N2}, P_I$ separate power ranges yielding qualitatively different behaviours.

sample remained circularly polarized. Let us notice that P^c_{th}, just like for unpolarized light, is twice the value of the threshold power for light linearly polarized parallel to the major axis of the intensity profile [9]. Above P^c_{th} the output beam became elliptically polarized, but the polarization ellipse remained steady. The optical-field-transition turned to be second order, contrary to the case of the circularly shaped beam [2] and it is about equal to the threshold value for unpolarized light for the same values of w_x and w_y. As the laser intensity increased, the molecular director moved out of the plane containing the major axis of the transverse beam profile. Above P_{N1}, the molecular director started to regularly nutate, i.e. to rotate in the transverse plane and contemporarily to oscillate in the meridian plane as shown in Figures 2–4. The nutation period is approximately independent of the incident power and is about 15 s. The transition from the steady state regime to nutational regime appeared to be an inverse Hopf bifurcation. As the laser intensity decreased from $P > P_{N1}$ to $P < P_{N1}$ the nutational regime switched off only after P had been brought significantly below P_{N1}. The hysteresis loop D-SN1-N-SN2 characterizes the intrinsic bistability effect in the absence of any bias static field. While the incident power remained below $P_I = (438 \pm 4)$ mW, no diffraction ring was observed in the far field except for a weak

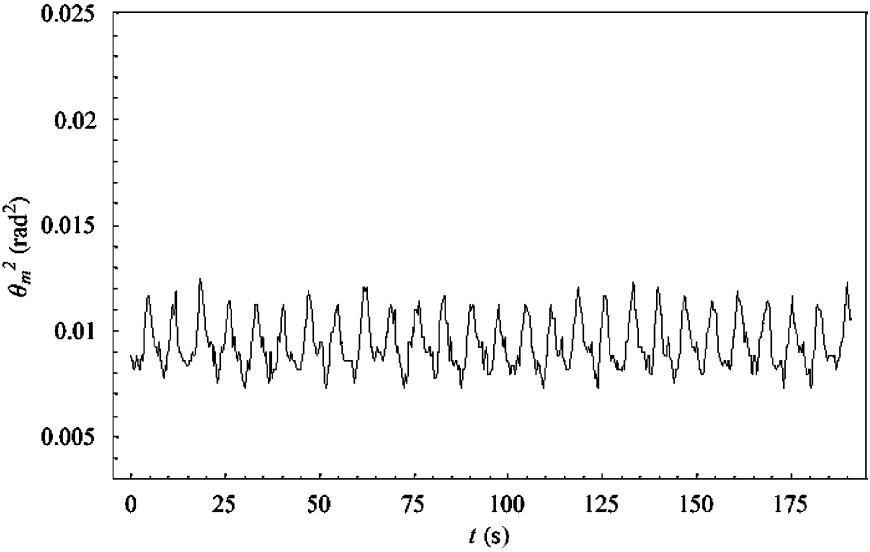

FIGURE 2 Persistent oscillations of θ_m^2 for circularly polarized light at $P = 371$ mW.

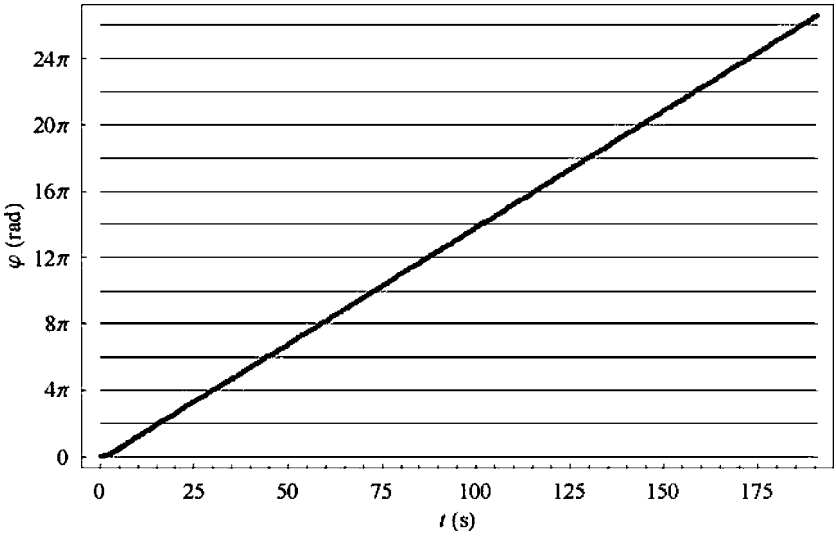

FIGURE 3 Rotation of the molecular director in the transverse plane for circularly polarized light at $P = 371$ mW.

halo. This, of course, indicates that the birefringence induced in the sample is so small that the phase difference between the ordinary and extraordinary waves accumulated in traversing the medium is less than π. Above the critical value P_I, the dynamical behaviour of the molecular director radically changed due to the rising of intermittent oscillations in the molecular nutation. This complex regime was recognized to be an on-off intermittency accompanied by chaotic rotation and has already been discussed in details elsewhere [13].

Let us focus the attention on the observations for $P < P_I$. The appearance of steady distorted states and the increasing of the threshold for SISLS can be explained in terms of the competition between the transfer of spin and orbital angular momentum of light [12]. Above the threshold for the optical Fréedericksz transition with circularly polarized input, the distribution of the molecular zenithal angle θ would tend to be aligned with the major axis of the intensity profile, since the optical field takes no privileged direction, as in the case of unpolarized light. In order to keep the elastic energy low, ϕ is likely to be along the major axis of θ-distribution and consequently along the major axis of the transverse beam profile. The medium then appears birefringent to the incoming beam and consequently the beam polarization becomes elliptical. Transfer of spin angular momentum from the beam to the medium would cause the molecular director to precess and then

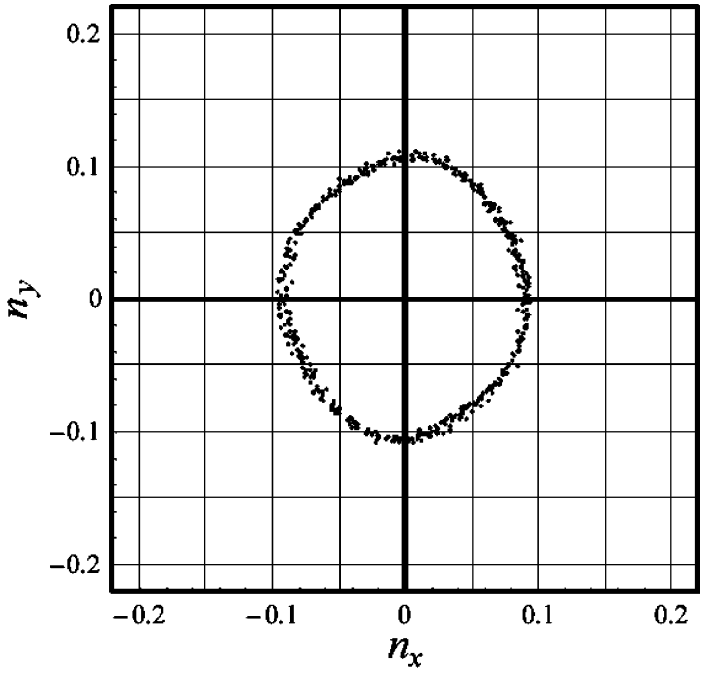

FIGURE 4 Periodic orbit of nutation of the molecular director at $P = 371$ mW.

the polarization ellipse following it, if the astigmatism of the transverse phase profile did not oppose it with a large enough transfer of orbital angular momentum. Theoretical calculations (see Fig. 5) show that, above threshold and till the incident power is below the critical value P_{N1}, the angular momentum transfer actually takes place and manages to close the balance of the total angular momentum, inhibiting the rotation of the molecular director in the same way as a brake. However as the incident power increases and the polarization inside the medium becomes more and more elliptical, thus lowering the threshold for the spin-induced rotation [19,20], the continually transferred spin angular momentum tends to drag the molecular director out of the plane containing the beam profile major axis (see Figs. 6 and 7). The leaving of the plane, driven by the spin, on one hand, stretches the spring connecting ϕ and γ, on the other hand, induces a restriction of the transverse phase profile (see Fig. 8). Since the strength of the spring does depend also on the degree of astigmatism of the θ-distribution, the elastic tie between γ and ϕ progressively

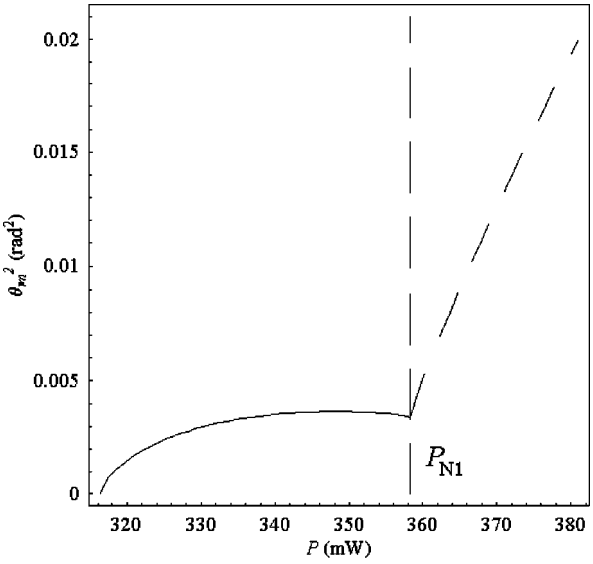

FIGURE 5 The time averaged value of θ_m^2 from the model. P_{N1} is the power for nutational transition. Below P_{N1} steady states are predicted. Dashed curve represents nutating states.

weakens as γ is leaving the plane. The process remains stationary while γ keeps close enough to the plane, so that the astigmatism of the effective lens is able to sustain the elastic interaction between γ and θ allowing for a transfer of orbital angular momentum large enough to balance the spin momentum transfer. A change in the dynamics then arises when the spring slackens due to the progressive decrease in the astigmatism of the transverse θ-distribution. The slackening of the spring causes ϕ and γ approximately to decouple so that ϕ is left free to rotate by the action of the spin transfer and γ to rotate back along the major axis of the beam profile due to orbital angular momentum transfer. For $P > P_{N1}$ the molecular director starts to nutate due to the superposition of the rotation of ϕ and the small oscillations of γ around the major axis of the beam profile. The oscillations of the phase distribution orientation then drive oscillations of θ_m^2, which is proportional to the phase change suffered by light traversing the sample. The model here adopted [12], however, gives no explanation for the hysteresis loop experimentally observed (see Fig. 1). This fault could be ascribed to the fact that the longitudinal twist distortion has not been accounted for. The hysteresis loop, in fact, can be qualitatively understood as follows. Decreasing the incident

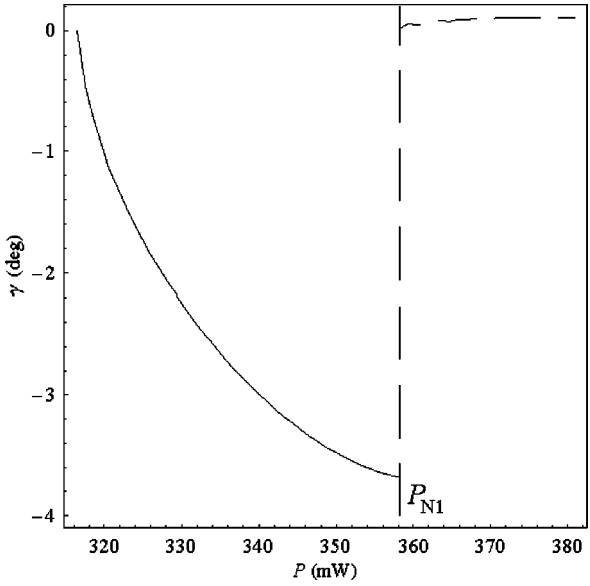

FIGURE 6 The time averaged value of γ from the model. P_{N1} is the power for nutational transition. Below P_{N1} steady states are predicted. Dashed curve represents nutating states.

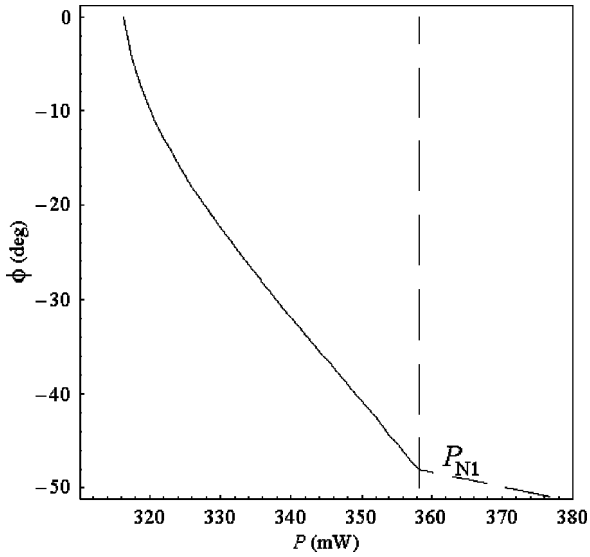

FIGURE 7 The time averaged value of ϕ from the model. P_{N1} is the power for nutational transition. Below P_{N1} steady states are predicted. Dashed curve represents nutating states.

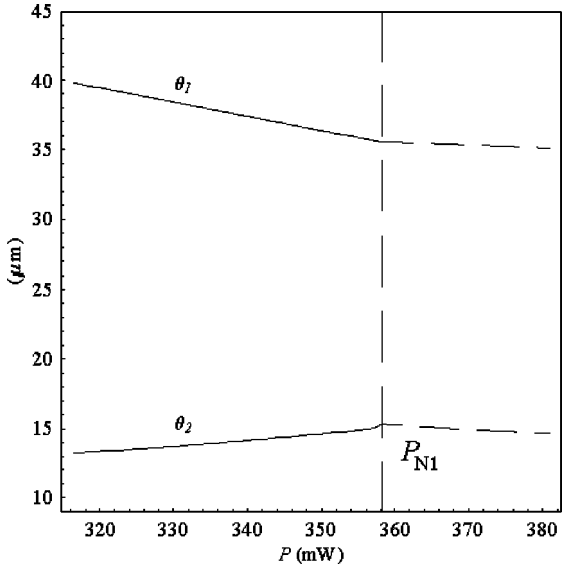

FIGURE 8 The time averaged value of θ_1 and θ_2 from the model. P_{N1} is the power for nutational transition. Below P_{N1} steady states are predicted. Dashed curve represents nutating states.

power from $P > P_{N1}$ to $P < P_{N1}$, the amount of spin angular momentum transferred to the medium tends to remain large and an equilibrium configuration may be only obtained for γ out enough of plane, which has been demonstrated to be an unstable state. Therefore, even slightly below P_{N1}, the molecular director may still nutate around the z-axis until the spin angular momentum transfer no longer overwhelms the braking action devolved by the orbital momentum, leading to the downward transition SN2-D. A large amount of spin transfer can be certainly sustained by a longitudinal torsional distortion in the sample, as it has been recently demonstrated [20]. The lacking of such a degree of freedom in the model used here could explain the absence of the experimentally observed hysteresis loop.

CONCLUSIONS

In this work, it has been shown that, in a homeotropically aligned NLC film irradiated by a circularly polarized laser beam, the symmetry breaking due to an elliptical beam shape significantly alters the well-known phenomenology of the optical reorientation observed using a beam with a circular cross-section. The observed changes have been

ascribed to the competition between the spin angular momentum transfer and the orbital angular momentum transfer induced by the non cylindrically-symmetric distortion suffered by molecules in the plane perpendicular to the beam propagation direction. It is well-known that no state of equilibrium is possible when a circularly polarized cylindrically-symmetric laser beam is used. In the case of an elliptically shaped laser beam, the symmetry breaking assists the formation, above the threshold, of steady distorted states, which are forbidden by circular symmetry. In these states spin and orbital angular momentum balance each other. As a consequence the OFT turns to be second rather than first order. The SISLS starts only after a second incident power threshold via an inverse Hopf bifurcation owing to the presence of hysteresis. The stimulated scattering turns to be associated to a nutational rather than precessional regime and, above a critical value for the incident power, intermittent oscillations arise in the molecular nutation. The delay in the SISLS start-up may be regarded as the effect due to a *braking* mechanism caused by the orbital angular momentum. New light-driven molecular motors could be envisaged involving an orbital angular momentum transfer. Part of the experimental results have been qualitatively explained in the light of the theoretical model worked out in Ref. [12]. A forthcoming work will be aimed at refining the theoretical predictions, introducing also a torsional degree of freedom, and, in particular, at explaining the complex dynamics observed at high incident power.

REFERENCES

[1] Beth, R. A. (1936). *Phys. Rev., 50*, 115.
[2] Santamato, E., Daino, B., Romagnoli, M., Settembre, M., & Shen, Y. R. (1986). *Phys. Rev. Lett., 57*, 2423.
[3] Marrucci, L., Abbate, G., Ferraiuolo, S., Maddalena, P., & Santamato, E. (1992). *Phys. Rev. A, 46*, 4859.
[4] Santamato, E., Abbate, G., Maddalena, P., Marrucci, L., & Shen, Y. R. (1990). *Phys. Rev. Lett., 64*, 1377.
[5] Santamato, E., Maddalena, P., Marrucci, L., & Piccirillo, B. (1998). *Liq. Cryst., 25*, 357.
[6] T. V. Galstyan & Drnoyan, V. (1997). *Phys. Rev. Lett., 78*, 2760.
[7] M. E. J. Friese, Nieminen, T. A., Heckenberg, N. R., & Rubinsztein-Dunlop, H. (1998). *Nature, 394*, 348.
[8] He, H., Friese, M. E. J., Heckenberg, N. R., & Rubinsztein-Dunlop, H. (1995). *Phys. Rev. Lett., 75*, 826.
[9] Piccirillo, B., Toscano, C., Vetrano, F., & Santamato, E. (2001). *Phys. Rev. Lett., 86*, 2285.
[10] Allen, L., Beijersbergen, M. W., Spreeuw, R. J. C., & Woerdman, J. P. (1992). *Phys. Rev. A, 45*, 8185.
[11] Piccirillo, B., Vella, A., & Santamato, E. (2004). *Phys. Rev. E, 69*, 021702.

[12] Piccirillo, B., Vella, A., & Santamato, E. (2002). *J. Opt. B: Quantum Semicl. Opt., 4*, S20.
[13] Vella, A., Setaro, A., Piccirillo, B., & Santamato, E. (2003). *Phys. Rev. E, 67*, 051704.
[14] Piccirillo, B. & Santamato, E. (2004). *Phys. Rev. E, 69*, 056613.
[15] Santamato, E., Romagnoli, M., Settembre, M., Daino, B., & Shen, Y. R. (1998). *Phys. Rev. Lett., 61*, 113.
[16] Zolot'ko, A. S., Kitaeva, V. F., Sobolev, N. N., & Sukhorukov, A. P. (1981). *Zh. Eksp. Teor. Fiz., 81*, 933 [*Sov. Phys.–JETP, 54*, 496 (1981)].
[17] Khoo, I. C., Liu, T. H., & Yan, P. Y. (1987). *J. Opt. Soc. Am. B, 4*, 115.
[18] Marrucci, L., Paparo, D., Vetrano, M. R., Colicchio, M., Santamato, E., & Viscardi, G. (2000). *J. Chem. Phys., 86*, 10361.
[19] Zel'dovich, B. Y. & Tabiryan, N. V. (1982). *Zh. Eksp. Teor. Fiz., 82*, 1126 [*Sov. Phys.–JETP 55*, 656 (1982)].
[20] Vella, A., Piccirillo, B., & Santamato, E. (2002). *Phys. Rev. E, 65*, 31706.